A high-throughput heterologous expression platform for plant synthetic biology based on Arabidopsis suspension cells

Lukas Meile[1,2,*], Germán Alonso-Tolo[1], Zeltia Ferreiro-Eiras[1], Xi Jiang[1], Stefan Burén[1], and Luis M. Rubio[1,*]

[1] Centro de Biotecnología y Genómica de Plantas, Universidad Politécnica de Madrid e Instituto Nacional de Investigación y Tecnología Agraria y Alimentaria/Consejo Superior de Investigaciones Científicas, Madrid 28223, Spain.

[2] Present address, Institute of Microbiology, ETH Zurich, 8093 Zurich, Switzerland.

**To whom correspondence should be addressed:* Luis M. Rubio: +34 910679189 – luis.rubio@csic.es; Lukas Meile lmeile@ethz.ch.

Other e-mail addresses: Germán Alonso-Tolo (german.atolo@upm.es), Zeltia Ferreiro-Eiras (zeltiaferreiroeiras@gmail.com), Xi Jiang (xi.jiang@upm.es), and Stefan Burén (stefan.buren@upm.es).

Word count: 3082 words and 6 Figures. Supplementary data: 6 figures and 4 supplementary tables.

Running title: High-Throughput Heterologous Expression in Arabidopsis Cells

Highlight (30 words max.)

We developed a fast and scalable expression platform in Arabidopsis suspension cells, enabling transient and stable multigene expression for applications in plant synthetic biology such as nitrogenase engineering.

Abstract (200 words max, graphical abstract possible)

Efficient heterologous expression platforms are essential for plant synthetic biology, particularly for engineering complex multigene pathways. Here, we establish a high-throughput system for both transient and stable transformation of *Arabidopsis thaliana* suspension cells using plant cell pack infiltration. This method requires no specialized equipment or consumables and is compatible with several cell lines. It enables rapid generation of 100 g of transgenic cells within two weeks and allows expression of at least 6 stacked genes from a single construct. We characterized constitutive promoters for gene expression in Arabidopsis cells and validated plastid targeting peptides. A library of NifB homologs was screened for expression and solubility and several archaeal variants suitable for plant expression were identified. We further engineered stable cell lines expressing up to six genes, encoding the NifB module components NifU, NifS, FdxN, and NifB, demonstrating that the newly developed platform integrates into an established workflow for nitrogenase engineering. The platform accelerates design–build–test cycles and facilitates the production of delicate proteins that require large amounts of transgenic biomass. It thus represents a versatile and scalable tool for advancing synthetic biology and for tackling major biotechnological challenges, such as biological nitrogen fixation.

Keywords (6-9, alphabetical order)

Arabidopsis thaliana transformation

Heterologous expression

Nitrogen fixation protein engineering

Plant biotechnology

Plant cell packs

Plant suspension cultures

Plant synthetic biology

Plastid protein expression

Protein solubility

Abbreviations

2,4-D	2,4-dichlorophenoxyacetic acid
BNF	biological nitrogen fixation
CTP	chloroplast targeting peptide
MS	Murashige and Skoog
NAA	1-naphthaleneacetic acid
PCP	plant cell pack
TS	Twin-Strep

Introduction

Plant cell suspension cultures provide a valuable system for heterologous protein production with several advantages over whole plants (Fischer *et al.*, 1999; Menges and Murray, 2004). They offer faster growth rates, simpler cultivation protocols, and reduced biological complexity due to a more uniform cell population. The homogeneous nature of suspension cultures facilitates reproducibility and scalability, which are essential for synthetic biology applications that require precise control over gene expression. Furthermore, the direct contact of all cells with the growth medium enables rapid and uniform exposure to external compounds such as expression inducers, signaling molecules, or nutrients. Together, these features make plant suspension cultures a powerful platform for accelerating design–build–test cycles in plant synthetic biology.

Several plant species have been employed for cell suspension-based expression, with tobacco (*Nicotiana tabacum*), rice (*Oryza sativa*), and carrot (*Daucus carota*) being the most widely used ones (Santos *et al.*, 2016). *Arabidopsis thaliana*, although used less frequently, offers some advantages that are yet to be fully exploited. As the most extensively studied model plant, Arabidopsis provides many genetic resources, including mutant collections and a well-annotated genome (Provart *et al.*, 2016). In addition, certain Arabidopsis cell lines retain the ability to form functional chloroplasts, allowing photomixotrophic growth (McCarthy *et al.*, 2016; Sello *et al.*, 2017) or even photoautotrophy when gradually reducing the external carbon source (Hampp *et al.*, 2012). Chloroplast development in suspension cells provides opportunities to study and engineer plastid-targeted proteins and chloroplast-related processes (Li *et al.*, 2021; McCarthy *et al.*, 2016; Sello *et al.*, 2016). Although Arabidopsis suspension cells have been used in various studies, and protocols for stable transformation and transient expression have been reported (Burén *et al.*, 2011; García-León *et al.*, 2018; Menges and Murray, 2004; Van Leene *et al.*, 2011), throughput and fast scalability remain limited. Furthermore, as for other plant systems, integration of multi-gene modules is still not a routine application (Rizzo *et al.*, 2023).

Engineering plants to fix atmospheric dinitrogen through direct transfer of prokaryotic nitrogen fixation (*nif*) genes is a key challenge of plant biotechnology (Curatti and Rubio, 2014; Oldroyd and Dixon, 2014). Nitrogenase is the prokaryotic multimeric metalloenzyme responsible for biological nitrogen fixation (BNF). Its function requires the coordinated expression of more than 10 Nif proteins, many of which are involved

in the biosynthesis of nitrogenase-specific essential Fe-S cofactors (Burén *et al.*, 2020). In addition to the high number of required Nif proteins, oxygen-sensitivity and low solubility of nitrogenase and other Nif proteins are major obstacles for engineering a functional plant nitrogenase (Burén and Rubio, 2018). Current strategies to engineer Nif proteins for eukaryotic expression have exploited the natural diversity of Nif proteins by systematically testing natural Nif protein variants for expression and solubility (Burén *et al.*, 2019; Jiang *et al.*, 2022; Jiang *et al.*, 2021).

The nitrogen fixation pathway can be divided into functional modules, each mediating an independent step of nitrogenase assembly. These modules can be optimized independently, reducing complexity and providing a tractable route toward full pathway reconstruction. Beyond optimizing protein expression, successful nitrogenase engineering is also thought to require subcellular targeting, with mitochondria and plastids being the two main candidate compartments. Mitochondria offer a favorable redox environment in which oxygen is consumed by respiration, but necessarily require protein import, which might be a limiting step for some Nif proteins (Oldroyd and Dixon, 2014). Plastids, by contrast, are genetically more accessible and support high expression levels (Boehm and Bock, 2019; Scotti *et al.*, 2012). Furthermore, reducing power is abundant in chloroplasts and plastid electron transport components are compatible with nitrogenase (Yang *et al.*, 2017). Although oxygen production during photosynthesis poses a major obstacle (Aznar-Moreno *et al.*, 2021; Eseverri *et al.*, 2020b; Ivleva *et al.*, 2016), strategies such as targeting non-photosynthetic plastids or temporally separating nitrogenase expression from photosynthesis have been proposed (Curatti and Rubio, 2014; Dixon *et al.*, 1997). In this context, Arabidopsis suspension cultures represent a particularly versatile model. They can be cultured under heterotrophic or photomixotrophic conditions, enabling studies on how oxygen production in chloroplasts affects Nif protein stability.

Biotechnological challenges such as nitrogenase engineering highlight the need for efficient platforms that allow iterative and flexible testing of complex biosynthetic pathways in plants. Here, we describe a platform for both transient and stable transformation of Arabidopsis suspension cells and demonstrate its utility by integrating it into an established workflow for nitrogenase engineering. We characterized a suite of constitutive promoters and performed expression and solubility screenings of a NifB library, providing new promising NifB candidates suitable for plant expression. We furthermore showed that the platform supports the stacking of at least six transgenes and allows quick scalability for protein purification. By enabling rapid protein production and synthetic pathway assembly in plant cells, this simple and low-cost platform contributes to advancing experimental approaches in plant synthetic biology.

Materials and methods

Plant cell lines and bacterial strains:

137 The Arabidopsis cell lines YG-1 and T87 were provided by the Riken Plant Cell Bank
138 (Yokohama, Japan). PSB-L cells were a gift from David Alabadí (IBMCP, Valencia,
139 Spain) and Col-0 and MM1 cells were a gift from Laszlo Bako (Umeå University,
140 Sweden). The *Escherichia coli* strain TOP10 was used for all cloning steps. The
141 *Agrobacterium tumefaciens* strain GV3101::pMP90 was a gift from Vicente Rubio and
142 used for PCP infiltration if not stated otherwise.

143 **Arabidopsis cell suspension cultures:**

144 Col-0 cells were routinely cultured in Murashige and Skoog (MS) medium including
145 vitamins with 3% sucrose, pH 5.7, supplemented with 2,4-dichlorophenoxyacetic acid
146 (2,4-D, 0.24 µg/ml) and kinetin (0.014 µg/ml) with weekly passages of 7 ml culture into
147 40 ml of fresh medium in 250-ml flasks. MM1 and PSB-L cells were routinely cultured
148 in 1x MS Basal Salts medium with 3% sucrose, pH 5.7, supplemented with thiamine
149 (0.4 µg/ml), myo-inositol (0.1 mg/ml), 1-naphthaleneacetic acid (NAA, 0.5 µg/ml) and
150 kinetin (0.05 µg/ml) with weekly passages of 2 ml culture into 48 ml of fresh medium
151 and 10 ml culture into 40 ml of fresh medium, respectively. YG-1 cells were cultured in
152 1x MS Basal Salts medium with 200 mg/L KH_2PO_4, 3% sucrose, pH 5.8, supplemented
153 with thiamine (0.4 µg/ml), myo-inositol (0.1 mg/ml), and 2,4-D (0.2 µg/ml) with weekly
154 passages of 5 ml sedimented cells into 40 ml of fresh medium. T87 cells were cultured
155 in MS medium including vitamins with 1.5% sucrose, pH 5.7, supplemented with NAA
156 (0.224 µg/ml) with biweekly passages of 1.2 ml of culture into 40 ml fresh medium. Col-
157 0 and YG-1 cells were routinely cultured at 25°C without light and MM1, PSB-L, and
158 T87 cells were cultured at 22°C under a 16-h photoperiod.

159 **Transient and stable plant cell transformation**:

160 The methods for transient and stable transformation of Arabidopsis suspension cells
161 are summarized in Fig. 1. Precultures for transient expression assays were prepared
162 as described above and grown for 3-7 days before transformation. Transient
163 expression assays were based on the plant cell pack (PCP) infiltration method
164 (Rademacher *et al.*, 2019). For PCP infiltration of Col-0, the medium was first removed
165 by pressing the tip of a serological pipette against the flask or tube bottom followed by
166 slow aspiration, similarly as described (Cortese *et al.*, 2021). The resulting compacted
167 cells were then resuspended in Paul's Medium (Buschmann, 2016) to a density that
168 barely allowed pipetting of the suspension with wide-bore tips. For small PCPs of
169 approximately 200 mg (fresh weight), 500 µl of cell suspension was loaded onto the
170 top part of 1000-µl filter pipette tips. The excess liquid was removed by vacuum for
171 approximately 10 s, resulting in PCP formation. *A. tumefaciens* suspensions were
172 prepared from 1-day-old precultures as described before (Gengenbach *et al.*, 2020),
173 but without acetosyringone, at OD_{600nm} 0.4 if not stated otherwise. PCPs were
174 infiltrated with 300 µl of *A. tumefaciens* suspension and incubated at 25°C for 1 h
175 before removing the excess liquid by vacuum for approximately 30 s. The infiltrated
176 PCPs were incubated inside a tip box equipped with sterile wet paper to maintain high
177 humidity for 2-4 days at 25°C in the dark, unless indicated otherwise.

For small-scale stable transformations of around 200 mg of starting biomass, PCPs were prepared the same way as for transient expression assays. For larger PCPs of approximately 8 g, cell suspensions were prepared similarly but 20 ml was loaded onto a Zymo-Spin V-PS midiprep column assembly (with the DNA-binding matrix removed) with a 15-ml Reservoir-X (Zymo Research, CA, USA). The excess medium was removed by gravity and 20 ml of *A. tumefaciens* suspension was passed through the packed cells by gravity. The excess liquid was removed by centrifugation in a swing-bucket rotor at 200 g for 2 min. The compacted, semi-dry PCPs were then transferred to a 50-ml centrifugation tube with a partially closed lid, sealed with Micropore tape (3M Health Care, USA) and incubated in a moist box. After 2-4 days, small PCPs were gently resuspended in 4 ml of cultivation medium described above containing carbenicillin (250 µg/ml) and vancomycin (165 µg/ml) to select against *A. tumefaciens*. For cell lines Col-0 and YG1, selection with hygromycin was applied at this point (20 µg/ml), whereas for MM1 hygromycin was only applied 2-3 days after resuspension. For large PCPs, cells were resuspended in 40 ml of growth medium, agitated on an orbital shaker at 100 rpm for 30 min before replacing the medium and supplementing with antibiotics as for small PCPs.

Plasmids, molecular cloning, gene library design and codon optimization:

Molecular cloning was performed using the Modular Cloning (MoClo) standard (Weber *et al.*, 2011; Werner *et al.*, 2012) as described before (Eseverri *et al.*, 2020b). For domestication of Level 0 parts, the Phusion Hot Start II DNA Polymerase (Thermo Fisher) was used with the primers and templates listed in Table S1. The sequence of all generated constructs used in this study was verified using a Sanger sequencing service (Macrogen, Madrid, Spain) or an Oxford Nanopore whole-plasmid sequencing service (Plasmidsaurus, Inc., Eugene, USA). All constructs and the individual parts used for their assembly are listed in Table S2. The MoClo Plant Parts Kit and pUAP1 were a gift from Nicola Patron (Addgene kit #1000000047, and plasmid #63674, respectively) and the MoClo Toolkit was a gift from Sylvestre Marillonnet (Addgene kit #1000000044). 35S:RUBY was a gift from Yunde Zhao (Addgene plasmid #160908) and pTHsp18.2 (GB0035) was a gift from Diego Orzaez (Addgene plasmid #68186). The *nifB* library was designed by keyword search in the Uniprot database (Bateman *et al.*, 2021). Archaeal NifB homologs were identified by discarding protein sequences lacking the six described NifB characteristic motifs (Arragain *et al.*, 2017), resulting in 321 candidate archaeal NifB homologs. Because Nif proteins from thermophilic organisms have been successfully expressed in eukaryotes before (Burén *et al.*, 2017; Jiang *et al.*, 2022), NifB homologs from thermophilic sources were considered as high-priority candidates. To identify them, NCBI taxon IDs associated with the Uniprot search results were used to obtain information on growth temperature and habitats in the Bac*Dive*, JGI IMG/D and GOLD databases (Chen *et al.*, 2021; Mukherjee *et al.*, 2025; Schober *et al.*, 2025). Furthermore, homologs from known diazotrophs were considered good candidates. Diverse source organisms were also considered by not including more than two homologs from the same taxonomic order. The workflow for the library design is summarized in Fig. S1. To improve expression in Arabidopsis, all

221 *nifB* sequences as well as the sequences of *nifU*, *nifS*, *fdxN*, and the TS-tag were
222 codon optimized using the DNA Chisel tool (Zulkower and Rosser, 2020). The
223 optimization constraints were high GC and GC3 contents of at least 50 and 69%,
224 respectively and avoiding BpiI, BsaI, and BsmBI restriction sites. The optimization
225 objectives included codon optimization for Arabidopsis, avoiding rare codons
226 (minimum frequency = 0.25), avoiding hairpins (stem size = 15, window = 200) as well
227 as avoiding the instability motifs considered by previous work (Eseverri *et al.*, 2020b).
228 The optimized sequences flanked by BsaI sites for cloning (Table S3) were ordered
229 from GenScript (USA).

230 **Luciferase reporter assay:**

231 Promoter activities were measured as previously reported (Li *et al.*, 2017) with
232 modifications. PCPs were lysed in a buffer containing 100 mM Tris-HCl (pH 8.6), 200
233 mM NaCl, 10% glycerol, 0.1% protease inhibitor cocktail (P9599, Sigma-Aldrich) with
234 4:1 (v/w) buffer/biomass ratio by metal bead (7 mm) beating in a Qiagen Retsch
235 MM300 TissueLyser for 60 s. Ten µl cell lysate was mixed with 100 µl luciferase buffer
236 containing 25 mM glycyl-glycine (pH 8), 14 mM K_2HPO_4-KH_2PO_4 (pH 8), 4 mM EGTA,
237 2 mM ATP, 1 mM DTT, 15 mM $MgSO_4$, 150 µg/ml D-luciferin in a white 96-well plate.
238 Luminescence was measured with an integration time of 2 s in a Varioskan LUX plate
239 reader (Thermo Scientific). For normalization of luciferase levels, every construct
240 contained the same GUS reporter cassette. GUS activity was measured in the same
241 device by mixing 10 µl cell lysate with 50 µl buffer containing 10 mM Tris-HCl (pH 8.0),
242 1 mM 4-methylumbelliferyl-β-D-glucuronide, and 2 mM $MgCl_2$ in a black 96-well plate.
243 The reaction was incubated at 37°C for 30 min with 100-ms measurements in 15-s
244 intervals with an excitation wavelength of 365 nm with a bandwidth of 12 nm and an
245 emission wavelength of 455 nm. The GUS activity was determined by calculating the
246 change in fluorescence over time in the linear phase. The promoter activity was
247 quantified by dividing the luminescence intensity by the GUS activity and normalized
248 to the strongest promoter of each run.

249 **Confocal microscopy:**

250 PCPs of the cell line Col-0 were infiltrated with *A. tumefaciens* harbouring the plasmids
251 1608-1614 (Table S2) as described above and harvested after 2 days by resuspension
252 in growth medium. Confocal laser scanning microscopy was performed with a Zeiss
253 LSM 880 microscope equipped with a Plan-Apochromat 40X/1.2 water-immersion
254 objective and 488-nm and 561-nm lasers. The detection ranges were 493-574 nm for
255 GFP and 578-696 nm for mCherry. Images were acquired using the ZEN 2.6 Black
256 software (Zeiss) and processed with the Fiji software (Schindelin *et al.*, 2012);
257 modifications included cropping, maximum-intensity projections, and adjustments of
258 brightness and contrast.

259 **Protein extraction, immunoblotting and purification:**

260 Protein extraction for immunoblotting was performed similarly as described (Burén *et*
261 *al.*, 2017) with modifications, if not stated otherwise. PCPs were added to a 2-ml

262 Eppendorf tube and subjected to 4 freeze-thaw cycles with liquid N_2. Lysis buffer,
263 containing 100 mM Tris-HCl (pH 8), 150 mM NaCl, 10 mM $MgCl_2$, 0.2% NP-40, 5%
264 glycerol, 5 mM β-mercaptoethanol, 5 mM EDTA, and 0.5% protease inhibitor cocktail
265 (Sigma P9599; added immediately before use), was added at a ratio of 2:1 (v/w) with
266 a 7-mm diameter steel ball and the cells were homogenized in a Qiagen Retsch
267 MM300 TissueLyser for 60 s, followed by a 15-min incubation at 4°C in a tube rotator.
268 The resulting homogenate was mixed at a ratio of 1:1 with 2x Laemmli buffer (125 mM
269 Tris-HCl pH 6.8, 4% SDS, 20% (v/v) glycerol, 10% β-mercaptoethanol, 0.005%
270 bromophenol blue) and heated for 10 min at 98°C, yielding the total cell extract. For
271 the soluble extract, the cell homogenate was centrifuged at 20,000 g for 15 min and
272 the supernatant containing the soluble proteins was treated with 2x Laemmli buffer as
273 described for the total extract. The heat-denatured protein samples were centrifuged
274 at 20,000 for 10 min before SDS-PAGE electrophoresis and immunoblotting. After
275 blotting, membranes were stained with a Ponceau S solution (0.2% in 5% acetic acid)
276 as transfer control. The Twin-Strep (TS) tag was detected with a monoclonal mouse
277 StrepII antibody (GenScript A01732, 1:5,000), NifU and NifS with rabbit polyclonal anti-
278 NifU and anti-NifS antibodies (Rubio lab, 1:20,000), the HA-tag with a rat monoclonal
279 antibody (Roche 12013819001, 1:5,000), GFP with a mouse monoclonal antibody
280 (Santa Cruz sc-9996, 1:2,000), and RbcL with a rabbit polyclonal antibody (Agrisera
281 AS03 037, 1:5,000). Secondary HRP-conjugated antibodies were used in 2% milk
282 powder in TBS-T diluted 1:20,000 (anti-mouse and anti-rabbit) or 1:5,000 (anti-rat).
283 NifB purifications were performed from Col-0 cells grown in the dark. Cells were
284 transformed with plasmid pN2LM282 as described above and scaled up to four 250-
285 ml shake flasks with 60 ml culture each. To collect cells, the grown transformant
286 cultures were bubbled with pure N_2 and then moved to an anaerobic chamber, where
287 the following steps were performed. Cells were harvested by filtration through a
288 ZymoPURE Syringe Filter-X (Zymo Research, CA, USA) followed by drying with tissue
289 paper and snap-freezing and storage in N_2. Cells were homogenized in a blender
290 (Oster Classic 4655) for 5 min at maximum speed with lysis buffer (100 mM Tris-HCl
291 [pH 8.6], 200 mM NaCl, 10% glycerol, 5 mM β-mercaptoethanol, 2 mM sodium
292 dithionite, 1 mM phenylmethylsulfonyl fluoride, 1 mg/ml leupeptin, 5 mg/ml DNase I)
293 with a buffer/biomass ratio of 2:1. The homogenate was then filtered through 2 layers
294 of miracloth. Lysate clearing, NifB purification and concentration was performed as
295 described (Jiang *et al.*, 2022), but with a 5-ml Strep-Tactin®XT 4Flow® column and a
296 peristaltic pump setup. Protein purity was assessed by SDS-PAGE analysis followed
297 by peptide mass fingerprinting of individual bands excised from the SDS-PAGE gel.
298 Mass spectrometry analysis was performed by a service of the Proteomic Unit at
299 Universidad Complutense de Madrid.

300

301 Results

302 A transient expression system for Arabidopsis suspension cells.

303 We first sought to improve the throughput of the *A. tumefaciens*-mediated transient
304 expression workflow for Arabidopsis suspension cells. The method was based on a
305 recently developed approach of plant cell pack (PCP) infiltration, which was originally
306 established for tobacco BY-2 cells (Rademacher *et al.*, 2019). For easy and individual
307 handling of PCPs, they were cast into the top part of filter pipette tips and the RUBY
308 (He *et al.*, 2020) and GFP reporters were used to assess successful transformation.
309 We first assessed four different *A. tumefaciens* strains for their suitability for PCP
310 infiltration with different Arabidopsis cell lines and found that the strain
311 GV3101::pMP90 led to RUBY expression in the cell line Col-0 (Fig. 2A) and YG-1 (Fig.
312 S2A), but not in the cell lines MM1, PSB-L, and T87 (Fig. 2A). Strain AGL-1 led to
313 RUBY expression in Col-0 but not in the other tested cell lines MM1, PSB-L, and T87
314 (Fig. 2A). Similarly, strain EHA105 led to RUBY expression only in Col-0 but not in the
315 other tested cells MM1 and PSB-L (Fig. S2A). Finally, PCPs infiltrated with the strain
316 LBA4404 never produced visible RUBY signal (Fig. 2A). The culture method of *A.*
317 *tumefaciens* did not affect infiltration success, as cultures grown in liquid or solid media
318 both led to RUBY expression (Fig. S2B). Since both Col-0 and YG-1 were routinely
319 cultured in darkness and the other cell lines under a 16-h photoperiod, we
320 hypothesized that cultivation under light might hamper transformation. Col-0 and MM1
321 cells grown either in darkness or under a 16-h photoperiod were then compared for
322 their receptiveness to PCP infiltration. MM1 cells grown under darkness were more
323 amenable to PCP infiltration; however, only small PCPs cast from 150 µl cell
324 suspension but not from 500 µl consistently yielded high transformation efficiency (Fig.
325 2A & D). A similar effect of light conditions on transformation efficiency was observed
326 for Col-0 cells, for which transformation was abolished when cultured under a 16-h
327 photoperiod (Fig. 2C).

328 Next, we tested whether Arabidopsis PCP infiltration can be improved by the co-
329 expression of the inhibitor of silencing p19. Co-expression of GFP and p19 in Col-0
330 PCPs was performed, either using a single *A. tumefaciens* strain harbouring both
331 genes on the same plasmid or using two co-infiltrated strains, each harbouring one of
332 the genes. To avoid the detection of GFP expressed in *A. tumefaciens* cells, which has
333 been described before (Buschmann, 2016), a *gfp* version containing the *DEM1* intron
334 (Christie *et al.*, 2011) was deployed. The p19 improved GFP expression irrespectively
335 of whether *gfp* and *p19* were present on the same plasmid or co-infiltrated (Fig. 2E).

336

337 **PCP infiltration is a fast method for generating stably transformed plant cells.**

338 We hypothesized that infiltrated PCPs could serve as an efficient source for stably
339 transformed cell cultures. This hypothesis was tested with the *A. tumefaciens* strain
340 GV3101::pMP90 because this strain has been successfully used for stable
341 transformation of Arabidopsis suspension cells (Burén *et al.*, 2011; García-León *et al.*,
342 2018). When resuspended in fresh culture medium amended with carbenicillin and
343 vancomycin to eliminate *A. tumefaciens*, PCPs carrying a hygromycin selection
344 cassette quickly formed a transgenic suspension culture under hygromycin selection,

345 as demonstrated by expression of the RUBY reporter (Fig. S2C-E). For the cell lines
346 Col-0 and MM1, transformation was possible with small PCPs of approximately 200
347 mg and 60 mg, respectively, as well as with large PCPs of approximately 8 g. The
348 transformation of large PCPs followed by hygromycin selection and scaling up the
349 culture allowed the production of nearly 100 g (fresh weight) of transformed Col-0 cells
350 within 13 days after PCP infiltration (Fig. S2D). Similarly to what was observed for
351 transient expression, the formation of transgenic lines from PCPs prepared from the
352 cell line MM1 was only consistently possible if the cells were grown under darkness
353 before infiltration (Fig. S2E). Furthermore, 2 days of co-culture with *A. tumefaciens*
354 yielded more consistent transformations than 3 days and an optical density of the
355 applied *A. tumefaciens* of 0.1 favoured transformation compared to a higher density of
356 0.4 (Fig. S2E).

357 **Characterization of a promoter set for heterologous expression in plant cells.**

358 To expand the molecular toolkit for synthetic biology applications including
359 heterologous expression from multigene constructs, we characterized 12 promoters
360 for constitutive gene expression in Arabidopsis suspension cells. A luciferase-based
361 reporter assay was used to measure promoter activity in infiltrated PCPs. The cassava
362 vein mosaic virus (CsVMV) promoter led to the highest luciferase expression and the
363 activity of the other promoters is therefore shown as percentage of the CsVMV activity
364 (Fig. 3). The widely used cauliflower mosaic virus *35S* (CMV35S) promoter exhibited
365 similar activity (96±16%), followed by the Arabidopsis ubitquitin-10 (*AtUbq10)* promoter
366 (73±3%) and the *A. tumefaciens* mannopine synthase (*AtuMas*) promoter (30±12%).
367 The tomato histone H4 (*SlH4*) promoter and the *A. tumefaciens* nopaline synthase
368 (*AtuNos*) promoters were considerably weaker (3±1% and 3±3%, respectively; Fig. 3).
369 The activities of the 6 weakest promoters were between 0.6±0.2% and 0.3±0.2%.
370 These findings suggest that the CsVMV, the CVM35S, the *AtUbq10*, and the *AtuMas*
371 promoters are most suitable for heterologous expression of proteins to be purified and
372 biochemically characterized in Arabidopsis suspension cells. The weaker promoters
373 can be used to drive the expression of accessory proteins that are required at lower
374 quantities.

375 **Solubility screening of plastid targeted proteins.**

376 We next sought to apply the newly established method for transient and stable
377 transformation of Arabidopsis suspension cells and the promoters validated for this
378 system to the engineering of BNF through heterologous expression of prokaryotic
379 nitrogen fixation (Nif) proteins. We aimed to identify new NifB protein variants that can
380 be used to engineer BNF in plants by performing a solubility screen of naturally
381 occurring NifB variants. Since NifB function and potentially also solubility depend on
382 the accessory proteins NifU, NifS and FdxN, we first generated a stable cell line
383 expressing those proteins to be used as a background line for the NifB solubility
384 screening. We therefore first tested a subset of the previously characterized promoters
385 and previously described chloroplast targeting peptides (CTPs) for expression and
386 plastid localization of NifU, NifS, and FdxN. NifX was co-expressed from the same

387 construct to test its solubility due to its function in nitrogenase co-factor biosynthesis
388 downstream of NifB. We found that the Arabidopsis *ubiquitin-10* promoter, the tomato
389 histone *H4* promoter and the Cassava Vein Mosaic Virus (CsVMV) promoter led to the
390 accumulation of NifU, NifS, and FdxN, respectively, in the soluble fraction of protein
391 extracts (Fig. 4A), whereas NifX was not soluble (Fig. S3). Since the latter protein is
392 not needed for NifB activity, *nifX* was excluded from later constructs. The Arabidopsis
393 CTPs from the TOCC, CAB6 and GLTB2 proteins allowed plastid localization, as
394 assessed by the presence of a single band in immunoblots, suggesting the absence of
395 full-length proteins with uncleaved CTPs (Fig. 4A), and by the co-localization of GFP-
396 fusion proteins with an established plastid marker protein, as determined by confocal
397 microscopy (Fig. 4B and Fig. S4). In a cell line that stably expressed NifU, NifS, and
398 FdxN, a library of 15 different *BCCP1::TS::nifB* homologs was tested in transient
399 expression assays (Fig. 5A), employing a TS-tag sequence that contains an intron to
400 avoid false positive detection resulting from misexpression in *A. tumefaciens*. Since
401 archaeal Nif variants have been successfully expressed in eukaryotes before, we
402 tested 13 *nifB* homologs from archaea and only two from bacteria. Two archaeal
403 homologs originated from uncultivated samples of extreme environments, the others
404 are from thermophilic and/or known diazotrophic archaea (Fig. 5B, Fig. S1, Table S4).
405 Comparing total and soluble extracts of *nifB*-infiltrated PCPs led to the accumulation
406 of soluble NifB protein for 11 out of 15 tested NifB homologs (Fig. 5C, Fig. S5). None
407 of the two tested bacterial NifB homologs were soluble in plant cells and only two of
408 the tested archaeal homologs were insoluble.

409 **Gene stacking and protein purification.**

410 To test the capacity of this method for stable expression of complex multi-gene
411 constructs, we generated Arabidopsis suspension cell lines carrying a single T-DNA
412 with six genes: a hygromycin resistance marker (*hygR*) for selection, *gfp* as a
413 transformation control, and the four gene components of the NifB module (*nifU*, *nifS*,
414 *fdxN*, and *nifB*). The construct design is shown in Fig. 6A. All four proteins were
415 detected in the soluble fraction of protein extracts from stably transformed cells by
416 immunoblotting (Fig. 6B), confirming successful expression. To further validate
417 expression and protein integrity, we performed affinity purification using a TS-tag fused
418 to NifB. Coomassie-stained gels of purification fractions revealed bands at the
419 expected size alongside some nonspecific background (Fig. 6C), and a Western blot
420 confirmed that NifB was specifically enriched during the purification (Fig. 6D).
421 Additional immunoblots for GFP and the plastid-localized RbcL protein confirmed the
422 release of both cytosolic and plastid contents during tissue homogenization. Mass
423 spectrometry confirmed the identity of the purified protein of the expected mass (39.5
424 kDa) as TS::NifB (Fig. S6). Together, these results demonstrate that our platform
425 supports large multi-gene constructs and simultaneous expression of several plastid-
426 targeted proteins in plant cells.

427

428 ## Discussion

429 In this study, we established and validated a rapid and efficient workflow for transient
430 and stable expression of multigene constructs in *A. thaliana* suspension cultures, with
431 the aim of enabling complex engineering tasks such as the reconstruction of the
432 nitrogen fixation pathway in plant cells. Our approach is based on the plant cell pack
433 infiltration method (Rademacher *et al.*, 2019) and adapts it for Arabidopsis,
434 demonstrating robust transformation efficiency, compatibility with several cell lines,
435 and rapid generation of stably transformed cultures. By applying this system to the
436 expression of plastid-targeted Nif proteins, we showcase its utility for synthetic biology
437 applications. A key innovation of this work is the combination of transient and stable
438 transformation workflows into a single streamlined platform. Unlike previous methods,
439 which require more than 40 days to yield 200 ml of transgenic cell cultures (García-
440 León *et al.*, 2018) or 29 days to yield 42 ml of culture (Van Leene *et al.*, 2011), the
441 workflow presented here can generate 300 ml transgenic culture containing 100 g of
442 cells in less than 2 weeks. This acceleration is probably due to a combination of a
443 higher amount of starting material and a higher transformation efficiency. The workflow
444 relies on basic low-cost equipment found in most biology laboratories. It significantly
445 increases experimental throughput, which is especially important for iterative testing of
446 multi-component systems like nitrogenase biosynthesis. Furthermore, transformed
447 cultures could be propagated without the need for selection, opening the way for simple
448 marker-less transformation applications.

449 While these features represent major advantages for plant synthetic biology, there are
450 also limitations to consider. The current workflow yields heterogeneous cell
451 populations rather than clonal lines, leading to varying T-DNA integration sites and
452 expression profiles. While this population-based approach suffices for solubility
453 screening and expression optimization, applications requiring precise genotype-
454 phenotype correlations may benefit from purified transgenic lines. However, isolating
455 and propagating individual Arabidopsis suspension cells is technically challenging due
456 to their requirement for high cell densities (Muir *et al.*, 1954). This constraint can be
457 addressed through the use “feeder cells” that maintain the growth of isolated
458 transformant cells or through microdroplet-based approaches, in which single cells are
459 cultured in small volumes (Schweiger *et al.*, 1987; Spangenberg and Koop, 1992). The
460 ability to isolate purified cell lines will also be critical for forward-genetic screens, which
461 are another possible future application of the presented platform thanks to the high
462 transformation efficiency combined with the possibility to generate stable
463 transformants. For example, bulk-transformations of fully assembled *nif* libraries could
464 be employed to select for nitrogenase activity using fluorescent H_2 or ethylene
465 biosensors in combination with fluorescence activated cell sorting.

466 The NifB solubility screen yielded results consistent with previous observations in
467 *Nicotiana benthamiana* leaves, supporting the use of Arabidopsis suspension cultures
468 as a relevant model system for plastid engineering. Specifically, the only three NifB
469 homologs that had been shown to be soluble in *N. benthamiana* leaves when targeted
470 to chloroplasts and/or mitochondria were also included in the library of the present
471 study and all of them were soluble in our Arabidopsis system. Notably, none of the 26

472 previously tested bacterial NifB homologs were soluble in *N. benthamiana* (Jiang *et al.*,
473 2022). Similarly, in the present study, none of the two tested bacterial NifB homologs
474 were soluble in Arabidopsis cells as opposed to 11 out of 13 tested archaeal homologs
475 that exhibited some level of solubility. This provides further evidence that archaeal Nif
476 variants might generally be superior for engineering BNF in eukaryotes.

477 This work lays the foundation for implementing multi-component pathways in plastids
478 and for exploring the effects of subcellular localization and nutrient availability on
479 nitrogenase stability and activity. Some Arabidopsis suspension cultures can be readily
480 shifted between heterotrophic and photomixotrophic conditions, enabling controlled
481 studies on the impact of photosynthetically produced oxygen on Nif protein
482 accumulation and function. However, not all cell lines are capable of consistently
483 developing chloroplasts even under light conditions, as shown for Col-0 (Fig. 2C);
484 therefore, the cell line MM1 would be more suitable to address research questions
485 related to chloroplast dynamics. This flexibility, in combination with high transformation
486 speed, makes the system highly suitable for prototyping nitrogenase expression
487 strategies and other complex biosynthetic pathways.

488

489 Supplementary data

490

491 Figure S1: *nifB* library design and homolog selection criteria.

492 Figure S2: Assessment of *A. tumefaciens* strain EHA105 and cell line YG1 for PCP
493 infiltration as well as examples of stable transformation of different cell lines.

494 Figure S3: NifX solubility testing.

495 Figure S4: Localization controls for confocal microscopy.

496 Figure S5: Additional replicate of NifB solubility screening.

497 Figure S6: NifB protein confirmation by mass spectrometry.

498 Table S1: Primers used in this study.

499 Table S2: Plasmids used in this study.

500 Table S3: Synthetic sequences ordered for this study.

501 Table S4: NifB library and corresponding source organisms.

502

503 Acknowledgements

504 We thank Álvaro Eseverri for help with MoClo assemblies, David Alabadí for providing
505 the cell line PSB-L, and Laszlo Bako for providing the cell lines Col-0 and MM1.

Author contributions

L.M., G.A.T., Z.F.E., X.J., and S.B. performed the experimental work, L.M., G.A.T., and L.M.R. designed experiments, analyzed data, and wrote the manuscript.

Conflict of interest

The authors declare no conflicts of interest.

Funding

This work was supported, in whole or in part, by the Gates Foundation grants INV-005889 and INV-067006. Under the grant conditions of the Foundation, a Creative Commons Attribution 4.0 License has already been assigned to the Author Accepted Manuscript version that might arise from this submission. L.M. was supported by the Swiss National Science Foundation grant P2EZP3_199998. G.A.T. was supported by Programa Propio UPM de I+D+i 2022.

Data availability

All data supporting the findings of this study are available within the paper and its Supplementary Information. A preprint version of the manuscript is available at bioRxiv under a CC BY 4.0 license.

References

Arragain S, Jiménez-Vicente E, Scandurra AA, Burén S, Rubio LM, Echavarri-Erasun C. 2017. Diversity and functional analysis of the FeMo-cofactor maturase NifB. Frontiers in Plant Science **8**.

Aznar-Moreno JA, Jiang X, Burén S, Rubio LM. 2021. Analysis of nitrogenase Fe protein activity in transplastomic tobacco. Frontiers in Agronomy **3**.

Bateman A, Martin MJ, Orchard S*, et al.* 2021. UniProt: the universal protein knowledgebase in 2021. Nucleic Acids Research **49**, D480–D489.

Boehm CR, Bock R. 2019. Recent advances and current challenges in synthetic biology of the plastid genetic system and metabolism. Plant Physiology **179**, 794–802.

Burén S, Jiang X, López-Torrejón G, Echavarri-Erasun C, Rubio LM. 2017. Purification and *in vitro* activity of mitochondria Targeted nitrogenase cofactor maturase NifB. Frontiers in Plant Science **8**.

Burén S, Jiménez-Vicente E, Echavarri-Erasun C, Rubio LM. 2020. Biosynthesis of nitrogenase cofactors. Chemical Reviews **120**, 4921–4968.

Burén S, Ortega-Villasante C, Blanco-Rivero A, Martínez-Bernardini A, Shutova T, Shevela D, Messinger J, Bako L, Villarejo A, Samuelsson G. 2011. Importance of post-translational modifications for functionality of a chloroplast-localized carbonic anhydrase (CAH1) in *Arabidopsis thaliana*. PLoS ONE **6**, e21021.

Burén S, Pratt K, Jiang X*, et al.* 2019. Biosynthesis of the nitrogenase active-site cofactor precursor NifB-co in *Saccharomyces cerevisiae*. Proceedings of the National Academy of Sciences of the United States of America **116**, 25078–25086.

Burén S, Rubio LM. 2018. State of the art in eukaryotic nitrogenase engineering. FEMS Microbiology Letters **365**, 274.

Buschmann H. 2016. Plant cell division analyzed by transient *Agrobacterium*-mediated transformation of tobacco BY-2 cells. Methods in molecular biology **1370**, 17–25.

Chen IMA, Chu K, Palaniappan K*, et al.* 2021. The IMG/M data management and analysis system v.6.0: new tools and advanced capabilities. Nucleic Acids Research **49**, D751–D763.

Christie M, Croft LJ, Carroll BJ. 2011. Intron splicing suppresses RNA silencing in Arabidopsis. The Plant Journal **68**, 159–167.

Cortese E, Carraretto L, Baldan B, Navazio L. 2021. Arabidopsis photosynthetic and heterotrophic cell suspension cultures. *Arabidopsis Protocols*, Vol. 2200: Springer US, 167–185.

Curatti L, Rubio LM. 2014. Challenges to develop nitrogen-fixing cereals by direct *nif*-gene transfer. Plant Science **225**, 130–137.

Dixon R, Cheng Q, Shen G-F, Day A, Dowson-Day M. 1997. *Nif* gene transfer and expression in chloroplasts: Prospects and problems. Plant and Soil **194**, 193–203.

Eseverri Á, Baysal C, Medina V, Capell T, Christou P, Rubio LM, Caro E. 2020a. Transit peptides from photosynthesis-related proteins mediate import of a marker protein into different plastid types and within different species. Frontiers in Plant Science **11**, 1.

Eseverri Á, López-Torrejón G, Jiang X, Burén S, Rubio LM, Caro E. 2020b. Use of synthetic biology tools to optimize the production of active nitrogenase Fe protein in chloroplasts of tobacco leaf cells. Plant Biotechnology Journal **18**, 1882–1896.

Fischer R, Emans N, Schuster F, Hellwig S, Drossard J. 1999. Towards molecular farming in the future: using plant-cell-suspension cultures as bioreactors. Biotechnology and Applied Biochemistry **30**, 109–112.

García-León M, Iniesto E, Rubio V. 2018. Tandem affinity purification of protein complexes from Arabidopsis cell cultures. *Two-Hybrid Systems*, Vol. 1794: Springer New York, 297–309.

Gengenbach BB, Opdensteinen P, Buyel JF. 2020. Robot cookies – plant cell packs as an automated high-throughput screening platform based on transient expression. Frontiers in Bioengineering and Biotechnology **8**.

Hampp C, Richter A, Osorio S, Zellnig G, Sinha AK, Jammer A, Fernie AR, Grimm B, Roitsch T. 2012. Establishment of a photoautotrophic cell suspension culture of *Arabidopsis thaliana* for photosynthetic, metabolic, and signaling studies. Molecular Plant **5**, 524–527.

He Y, Zhang T, Sun H, Zhan H, Zhao Y. 2020. A reporter for noninvasively monitoring gene expression and plant transformation. Horticulture Research **7**, 1–6.

Ivleva NB, Groat J, Staub JM, Stephens M. 2016. Expression of active subunit of nitrogenase via integration into plant organelle genome. PLoS ONE **11**, e0160951.

Jiang X, Coroian D, Barahona E, Echavarri-Erasun C, Castellanos-Rueda R, Eseverri Á, Aznar-Moreno JA, Burén S, Rubio LM. 2022. Functional nitrogenase cofactor maturase NifB in mitochondria and chloroplasts of *Nicotiana benthamiana*. mBio **13**.

Jiang X, Payá-Tormo L, Coroian D, García-Rubio I, Castellanos-Rueda R, Eseverri Á, López-Torrejón G, Burén S, Rubio LM. 2021. Exploiting genetic diversity and gene synthesis to identify superior nitrogenase NifH protein variants to engineer N_2-fixation in plants. Communications Biology **4**, 1–11.

Li C, Liu Y, Liu X*, et al.* 2021. Chloroplast thylakoid ascorbate peroxidase PtotAPX plays a key role in chloroplast development by decreasing hydrogen peroxide in *Populus tomentosa*. Journal of Experimental Botany **72**, 4333–4354.

Li Z, Zhang D, Xiong X, Yan B, Xie W, Sheen J, Li JF. 2017. A potent Cas9-derived gene activator for plant and mammalian cells. Nature Plants 2017 3:12 **3**, 930–936.

McCarthy A, Chung M, Ivanov AG, Krol M, Inman M, Maxwell DP, Hüner NPA. 2016. An established *Arabidopsis thaliana* var. Landsberg *erecta* cell suspension culture accumulates chlorophyll and exhibits a stay-green phenotype in response to high external sucrose concentrations. Journal of Plant Physiology **199**, 40–51.

Menges M, Murray JAH. 2004. Cryopreservation of transformed and wild-type *Arabidopsis* and tobacco cell suspension cultures. The Plant Journal **37**, 635–644.

Muir WH, Hildebrandt AC, Riker AJ. 1954. Plant tissue cultures produced from single isolated cells. Science **119**, 877–878.

Mukherjee S, Stamatis D, Cindy*, et al.* 2025. Genomes OnLine Database (GOLD) v.10: new features and updates. Nucleic Acids Research **53**, D989–D997.

Oldroyd GE, Dixon R. 2014. Biotechnological solutions to the nitrogen problem. Current Opinion in Biotechnology **26**, 19–24.

Provart NJ, Alonso J, Assmann SM*, et al.* 2016. 50 years of Arabidopsis research: highlights and future directions. New Phytologist **209**, 921–944.

Rademacher T, Sack M, Blessing D, Fischer R, Holland T, Buyel J. 2019. Plant cell packs: a scalable platform for recombinant protein production and metabolic engineering. Plant Biotechnology Journal **17**, 1560.

Rizzo P, Chavez BG, Leite Dias S, D'Auria JC. 2023. Plant synthetic biology: from inspiration to augmentation. Current Opinion in Biotechnology **79**, 102857.

Santos RB, Abranches R, Fischer R, Sack M, Holland T. 2016. Putting the spotlight back on plant suspension cultures. Frontiers in Plant Science **7**.

Schindelin J, Arganda-Carreras I, Frise E*, et al.* 2012. Fiji: an open-source platform for biological-image analysis. Nature Methods **9**, 676–682.

Schober I, Koblitz J, Joaquim*, et al.* 2025. Bac*Dive* in 2025: the core database for prokaryotic strain data. Nucleic Acids Research **53**, D748–D756.

Schweiger HG, Dirk J, Koop HU, Kranz E, Neuhaus G, Spangenberg G, Wolff D. 1987. Individual selection, culture and manipulation of higher plant cells. Theoretical and Applied Genetics **73**, 769–783.

Scotti N, Rigano MM, Cardi T. 2012. Production of foreign proteins using plastid transformation. Biotechnology Advances **30**, 387–397.

Sello S, Moscatiello R, La Rocca N, Baldan B, Navazio L. 2017. A rapid and efficient method to obtain photosynthetic cell suspension cultures of *Arabidopsis thaliana*. Frontiers in Plant Science **8**, 1–8.

Sello S, Perotto J, Carraretto L, Szabò I, Vothknecht UC, Navazio L. 2016. Dissecting stimulus-specific Ca^{2+} signals in amyloplasts and chloroplasts of *Arabidopsis thaliana* cell suspension cultures. Journal of Experimental Botany **67**, 3965–3974.

Spangenberg G, Koop HU. 1992. Low density cultures: microdroplets and single cell nurse cultures. *Plant Tissue Culture Manual*: Kluwer Academic Publishers, 51–78.

Van Leene J, Eeckhout D, Persiau G, Van De Slijke E, Geerinck J, Van Isterdael G, Witters E, De Jaeger G. 2011. Isolation of transcription factor complexes from *Arabidopsis* cell suspension cultures by tandem affinity purification. *Plant transcription factors*: Humana Press, 195–218.

Weber E, Engler C, Gruetzner R, Werner S, Marillonnet S. 2011. A modular cloning system for standardized assembly of multigene constructs. PLoS ONE **6**, 16765.

Werner S, Engler C, Weber E, Gruetzner R, Marillonnet S. 2012. Fast track assembly of multigene constructs using golden gate cloning and the MoClo system. Bioengineered Bugs **3**, 38–43.

Yang J, Xie X, Yang M, Dixon R, Wang Y-P. 2017. Modular electron-transport chains from eukaryotic organelles function to support nitrogenase activity. Proceedings of the National Academy of Sciences **114**, E2460–E2465.

Zulkower V, Rosser S. 2020. DNA Chisel, a versatile sequence optimizer. Bioinformatics **36**, 4508–4509.

Figure Legends

Fig 1: Workflow and applications of plant cell pack (PCP) infiltration in Arabidopsis suspension cells for stable and transient transformation at different scales. (A) Plant cells are maintained by weekly or monthly passaging in liquid or solid MS medium, respectively. Washed plant cells grown in liquid medium under darkness serve as starting material for both transient and stable transformations. 200-mg PCPs allow high throughput, whereas 8-g PCPs allow the production of up to 100 g (fresh weight) of transgenic cells in 2 weeks. (B) For high-throughput applications, a dense suspension of washed cells is loaded on top of a pipette filter tip. The excess liquid is then removed by vacuum and the semi-dry PCP is infiltrated with an *A. tumefaciens* suspension. After 60 min, the excess liquid is removed and the PCPs show transgene expression after 2-3 days. Individual PCPs can be conveniently transferred to microcentrifuge tubes downstream applications such as protein extraction, microscopy, or the generation of stably transformed cells. (C) For high-volume applications such as the purification of heterologously produced proteins, washed suspension cells are loaded onto midi-prep columns and excess liquid is removed by gravity or gentle vacuum. *A. tumefaciens* is loaded by gravity and, after 60 min, excess liquid and bacteria are removed by gentle centrifugation and PCPs are transferred to 50-ml centrifugation tubes. After 2-3 days, transformed PCPs are resuspended in fresh medium to start a liquid culture. Created in https://BioRender.com.

Fig 2: Optimization of transient expression in Arabidopsis suspension cells by plant cell pack (PCP) infiltration. (A) PCPs of four different Arabidopsis cell lines infiltrated with three different *A. tumefaciens* strains harboring a plasmid with the RUBY reporter. Pictures were taken 2 and 3 days post infiltration (dpi). PCPs treated with the infiltration buffer only were included as negative control. (B) PCPs of the Arabidopsis cell line Col-0 infiltrated with the *A. tumefaciens* strain GV3101::pMP90 carrying the RUBY cassette prepared from liquid or solid culture medium. (C) PCPs from the cell line Col-0 grown either under constant darkness or a 16-h photoperiod and infiltrated with *RUBY*-carrying *A. tumefaciens* strain GV3101::pMP90 (+) or with infiltration buffer only (-). (D) PCP infiltration of cell line MM1 grown either under darkness or a 16-h photoperiod with RUBY-carrying *A. tumefaciens* strain GV3101::pMP90 prepared at different optical densities (+) or with infiltration buffer only (-). (E) Co-expression of the suppressor of silencing P19 driven by the *Nos* promoter and GFP driven by the *35S* promoter in PCPs of cell line Col-0. The *p19* and *gfp* genes were either present on the same or on different plasmids. Three technical replicates are shown.

Fig 3: Various constitutive promoters of different strength allow transgene expression in Arabidopsis suspension cells. Relative promoter activity as determined by LUC reporter assays. Different constitutive promoters driving expression the firefly luciferase (*fluc*) gene were co-transformed with a GUS reporter cassette (*p35S::GUS::t35S*) for normalization and the suppressor of silencing *p19* from a single T-DNA (grey box; not to scale). Promoter activity was defined as luminescence divided by GUS activity. Bars show the average of 3 biological replicates. The y-axis is segmented with two different scales. Individual replicates are shown as black dots

and error bars represent the standard deviation. Letters represent statistical groups according to one-way ANOVA and Tukey's test. LB: left T-DNA border; RB: right T-DNA border.

Fig 4: Soluble proteins of the NifB functional module can be expressed and targeted to plastids in Arabidopsis suspension cells. (A) Western blots of total and soluble plant cell extracts transformed with *nifU*, *nifS*, and *fdxN* driven by the Arabidopsis *ubiquitin-10* promoter, the tomato histone H4 promoter, and the Cassava Vein Mosaic Virus (CsVMV) promoter, respectively. The proteins were fused to minimal versions of the chloroplast-targeting peptides (CTPs) of the Arabidopsis proteins TOCC, CAB6, and GLTB2, respectively (Eseverri *et al.*, 2020a). FdxN was fused to an HA-tag for detection, whereas NifU and NifS were untagged. Col-0 cells were transformed with plasmid pN2LM165 (rep1) and plasmid pN2LM166 (rep2) and proteins extracted with a buffer containing 100 mM Tris-HCl (pH8), 150mM NaCl, 10% glycerol and 0.5% protease inhibitor cocktail. (B) Detection of GFP signal in Arabidopsis cells transformed with *nifU*, *nifS* and *fdxN* fused to *gfp* and the TOCC, CAB6 and GLTB2 CTPs, respectively, by confocal laser scanning microscopy. The mCherry reporter fused to the RecA CTP was used as a control for plastid localization. Merged pictures of the mCherry and GFP channels are also shown. Scale bars: 10 µm.

Fig 5: Solubility screening identified new archaeal NifB protein variants suitable for plant expression. (A) Construct and expression design for the NifB solubility screening. A stably transformed background line expressing *nifU*, *nifS*, and *fdxN::HA* was generated first. In this background line, the different *nifB* homologs fused to the BCCP1 chloroplast targeting peptide (Eseverri *et al.*, 2020b) were transiently co-expressed with *gfp* as a transformation control and the suppressor of silencing p19. (B) Workflow overview for the *nifB* library and synthetic gene design. NifB variants annotated by Uniprot were filtered for known NifB protein motifs (Arragain *et al.*, 2017) and for archaeal origin. Public databases such as Bac*Dive* (Schober *et al.*, 2025) and information on isolation sources were used to select 8 NifB homologs from thermophilic organisms. Additionally, four homologs from known diazotrophic archaea, one from an uncultured archaeon, and two from extremophilic bacteria were included. The synthetic gene design was performed using the DNA Chisel program (Zulkower and Rosser, 2020), focusing on matching the codon usage to Arabidopsis and obtaining high GC and GC3 content as well as avoiding known mRNA instability motifs. (C) Western blots of total (T) and soluble (S) plant cell extracts. NifB variants were fused to the Twin-Strep (TS) tag for detection with a Strep monoclonal antibody (StrepMAB). A control with the same expression vector but without *nifB* was included (-NifB). LB: left T-DNA border; RB: right T-DNA border; CTP: chloroplast targeting peptide; *hygR*: hygromycin selection marker.

Fig 6: Multi-gene stacking of the NifB module in stably transformed plant cells. (A) Construct design for stable transformation for expression plastid-targeted NifU, NifS, FdxN::HA, Twin-Strep::NifB, and cytosolic GFP. CTP: chloroplast targeting peptide (B) Western blots and ponceau-stained membranes of total and soluble plant

extracts from MM1 plant cells transformed with the construct depicted in (A) with *nifB* from *Methanobacterium bryantii*, using α-NifU, α-NifS, α-HA, α-StrepII and α-GFP antibodies. (C) Left panel: Coomassie-stained SDS-PAGE gel loaded with different fractions of the Strep-Tactin affinity chromatographic purification of Col-0 cells transformed with the construct depicted in (A) with *nifB* from *Methanosarcina acetivorans*. Asterisk indicates the expected mass of TS-NifB, 39.5 kDa. Right panel: concentrated elution. Bands labelled with red numbers were analyzed by mass spectrometry. Band 3 was identified as TS::NifB, whereas bands 1, 2, and 4 corresponded to co-purified Arabidopsis proteins methylcrotonoyl-CoA carboxylase subunits alpha (Q42523) and beta (Q9LDD8), and the biotin carboxyl carrier protein of acetyl-CoA carboxylase (F4KE21), respectively. Band 5 was identified as a mix of the Arabidopsis proteins A0A384KVD0 and Q9SSR9 of unknown functions. (D) Western blots of the purification steps shown in (C) with the α-Strep (StrepMAB), α-RbcL, α-GFP antibodies.

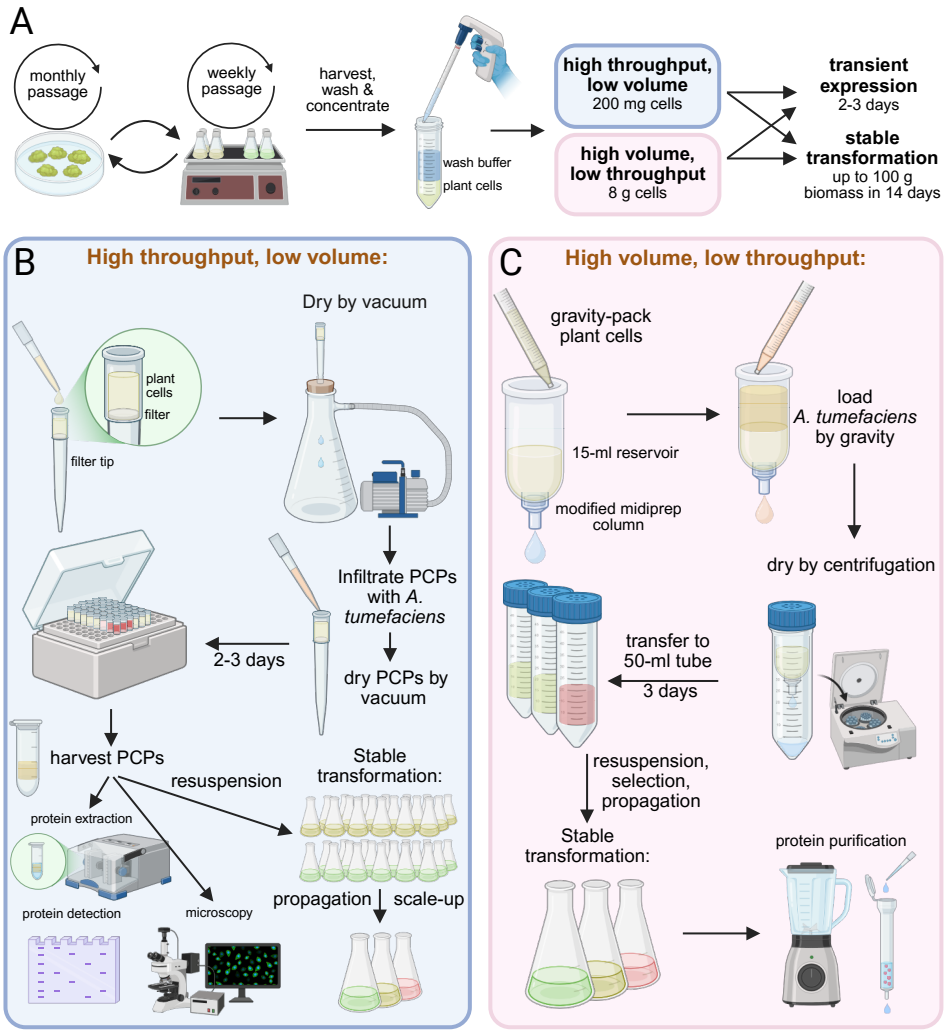

Fig 1: Workflow and applications of plant cell pack (PCP) infiltration in Arabidopsis suspension cells for stable and transient transformation at different scales. (A) Plant cells are maintained by weekly or monthly passaging in liquid or solid MS medium, respectively. Washed plant cells grown in liquid medium under darkness serve as starting material for both transient and stable transformations. 200-mg PCPs allow high throughput, whereas 8-g PCPs allow the production of up to 100 g (fresh weight) of transgenic cells in 2 weeks. (B) For high-throughput applications, a dense suspension of washed cells is loaded on top of a pipette filter tip. The excess liquid is then removed by vacuum and the semi-dry PCP is infiltrated with an *A. tumefaciens* suspension. After 60 min, the excess liquid is removed and the PCPs show transgene expression after 2-3 days. Individual PCPs can be conveniently transferred to microcentrifuge tubes downstream applications such as protein extraction, microscopy, or the generation of stably transformed cells. (C) For high-volume applications such as the purification of heterologously produced proteins, washed suspension cells are loaded onto midi-prep columns and excess liquid is removed by gravity or gentle vacuum. *A. tumefaciens* is loaded by gravity and, after 60 min, excess liquid and bacteria are removed by gentle centrifugation and PCPs are transferred to 50-ml centrifugation tubes. After 2-3 days, transformed PCPs are resuspended in fresh medium to start a liquid culture. Created in https://BioRender.com.

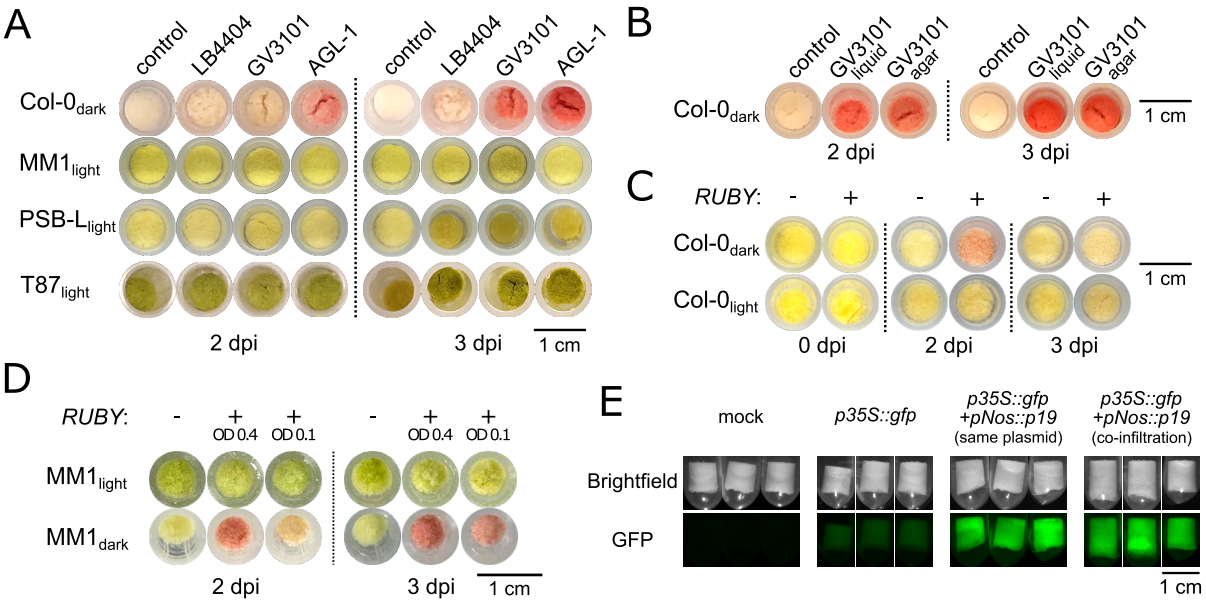

Fig 2: Optimization of transient expression in Arabidopsis suspension cells by plant cell pack (PCP) infiltration. (A) PCPs of four different Arabidopsis cell lines infiltrated with three different *A. tumefaciens* strains harboring a plasmid with the RUBY reporter. Pictures were taken 2 and 3 days post infiltration (dpi). PCPs treated with the infiltration buffer only were included as negative control. (B) PCPs of the Arabidopsis cell line Col-0 infiltrated with the *A. tumefaciens* strain GV3101::pMP90 carrying the RUBY cassette prepared from liquid or solid culture medium. (C) PCPs from the cell line Col-0 grown either under constant darkness or a 16-h photoperiod and infiltrated with *RUBY*-carrying *A. tumefaciens* strain GV3101::pMP90 (+) or with infiltration buffer only (-). (D) PCP infiltration of cell line MM1 grown either under darkness or a 16-h photoperiod with RUBY-carrying *A. tumefaciens* strain GV3101::pMP90 prepared at different optical densities (+) or with infiltration buffer only (-). (E) Co-expression of the suppressor of silencing P19 driven by the *Nos* promoter and GFP driven by the *35S* promoter in PCPs of cell line Col-0. The *p19* and *gfp* genes were either present on the same or on different plasmids. Three technical replicates are shown.

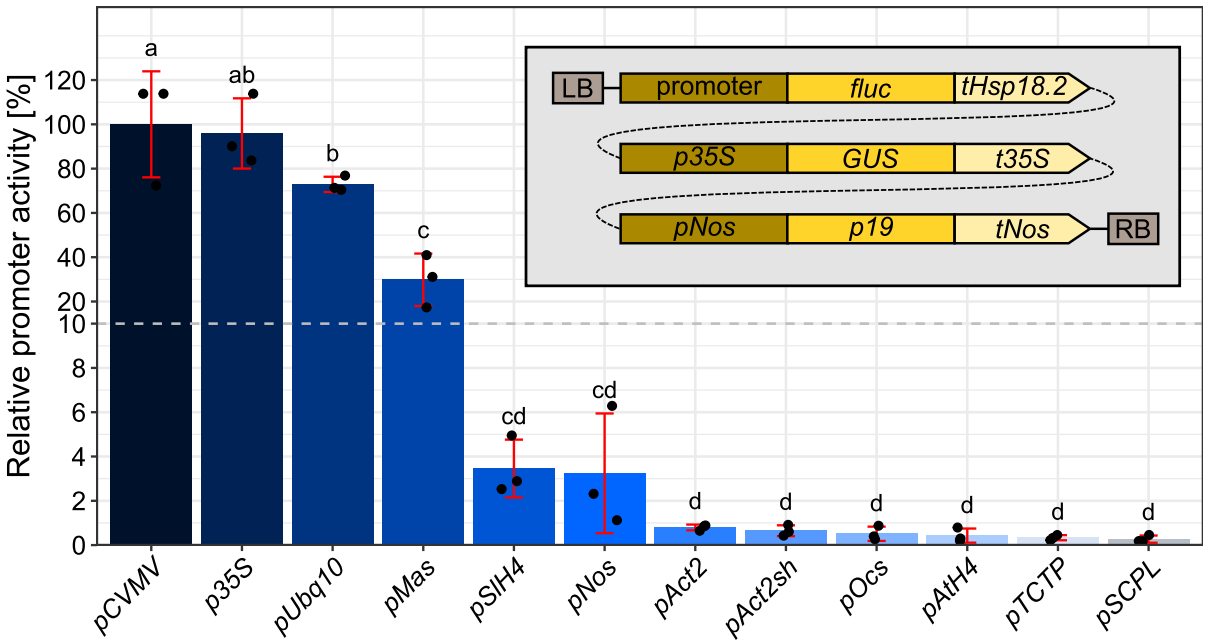

Fig 3: Various constitutive promoters of different strength allow transgene expression in Arabidopsis suspension cells. Relative promoter activity as determined by LUC reporter assays. Different constitutive promoters driving expression the firefly luciferase (*fluc*) gene were co-transformed with a GUS reporter cassette (*p35S::GUS::t35S*) for normalization and the suppressor of silencing *p19* from a single T-DNA (grey box; not to scale). Promoter activity was defined as luminescence divided by GUS activity. Bars show the average of 3 biological replicates. The y-axis is segmented with two different scales. Individual replicates are shown as black dots and error bars represent the standard deviation. Letters represent statistical groups according to one-way ANOVA and Tukey's test. LB: left T-DNA border; RB: right T-DNA border.

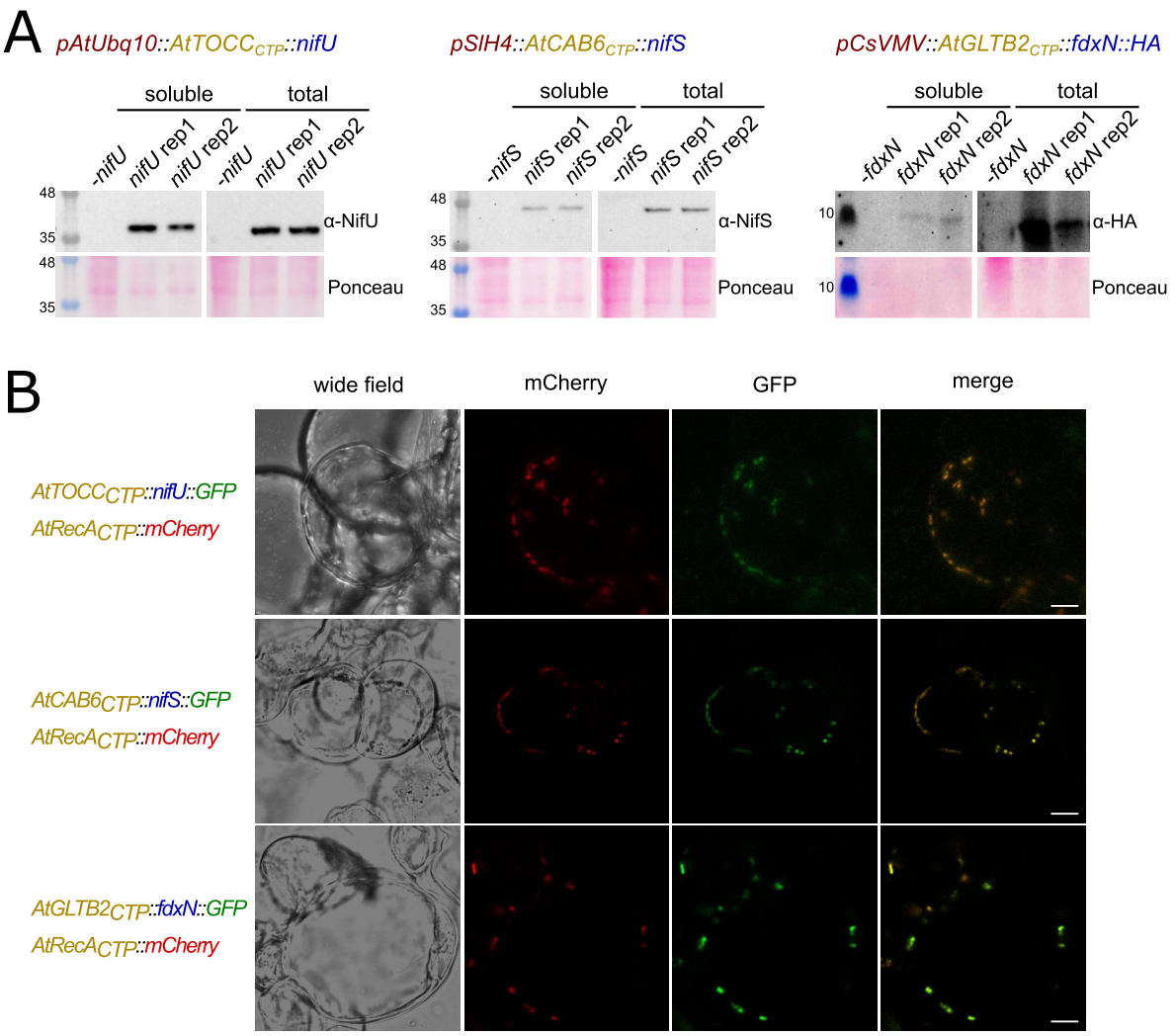

Fig 4: Soluble proteins of the NifB functional module can be expressed and targeted to plastids in Arabidopsis suspension cells. (A) Western blots of total and soluble plant cell extracts transformed with *nifU*, *nifS*, and *fdxN* driven by the Arabidopsis *ubiquitin-10* promoter, the tomato histone H4 promoter, and the Cassava Vein Mosaic Virus (CsVMV) promoter, respectively. The proteins were fused to minimal versions of the chloroplast-targeting peptides (CTPs) of the Arabidopsis proteins TOCC, CAB6, and GLTB2, respectively (Eseverri *et al.*, 2020a). FdxN was fused to an HA-tag for detection, whereas NifU and NifS were untagged. Col-0 cells were transformed with plasmid pN2LM165 (rep1) and plasmid pN2LM166 (rep2) and proteins extracted with a buffer containing 100 mM Tris-HCl (pH8), 150mM NaCl, 10% glycerol and 0.5% protease inhibitor cocktail. (B) Detection of GFP signal in Arabidopsis cells transformed with *nifU*, *nifS* and *fdxN* fused to *gfp* and the TOCC, CAB6 and GLTB2 CTPs, respectively, by confocal laser scanning microscopy. The mCherry reporter fused to the RecA CTP was used as a control for plastid localization. Merged pictures of the mCherry and GFP channels are also shown. Scale bars: 10 µm.

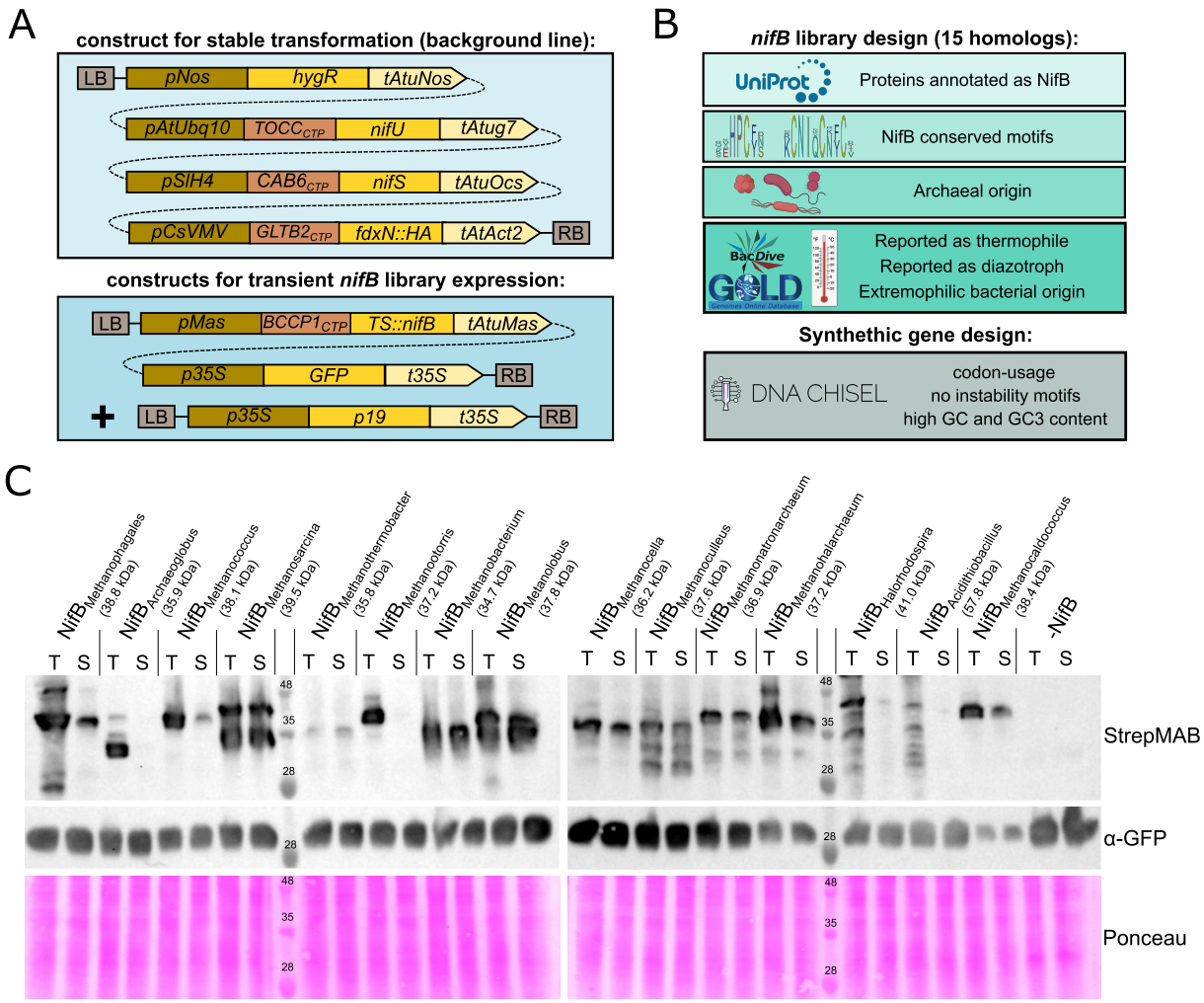

Fig 5: Solubility screening identified new archaeal NifB protein variants suitable for plant expression. (A) Construct and expression design for the NifB solubility screening. A stably transformed background line expressing *nifU*, *nifS*, and *fdxN::HA* was generated first. In this background line, the different *nifB* homologs fused to the BCCP1 chloroplast targeting peptide (Eseverri *et al.*, 2020b) were transiently co-expressed with *gfp* as a transformation control and the suppressor of silencing p19. (B) Workflow overview for the *nifB* library and synthetic gene design. NifB variants annotated by Uniprot were filtered for known NifB protein motifs (Arragain *et al.*, 2017) and for archaeal origin. Public databases such as Bac*Dive* (Schober *et al.*, 2025) and information on isolation sources were used to select 8 NifB homologs from thermophilic organisms. Additionally, four homologs from known diazotrophic archaea, one from an uncultured archaeon, and two from extremophilic bacteria were included. The synthetic gene design was performed using the DNA Chisel program (Zulkower and Rosser, 2020), focusing on matching the codon usage to Arabidopsis and obtaining high GC and GC3 content as well as avoiding known mRNA instability motifs. (C) Western blots of total (T) and soluble (S) plant cell extracts. NifB variants were fused to the Twin-Strep (TS) tag for detection with a Strep monoclonal antibody (StrepMAB). A control with the same expression vector but without *nifB* was included (-NifB). LB: left T-DNA border; RB: right T-DNA border; CTP: chloroplast targeting peptide; *hygR*: hygromycin selection marker.

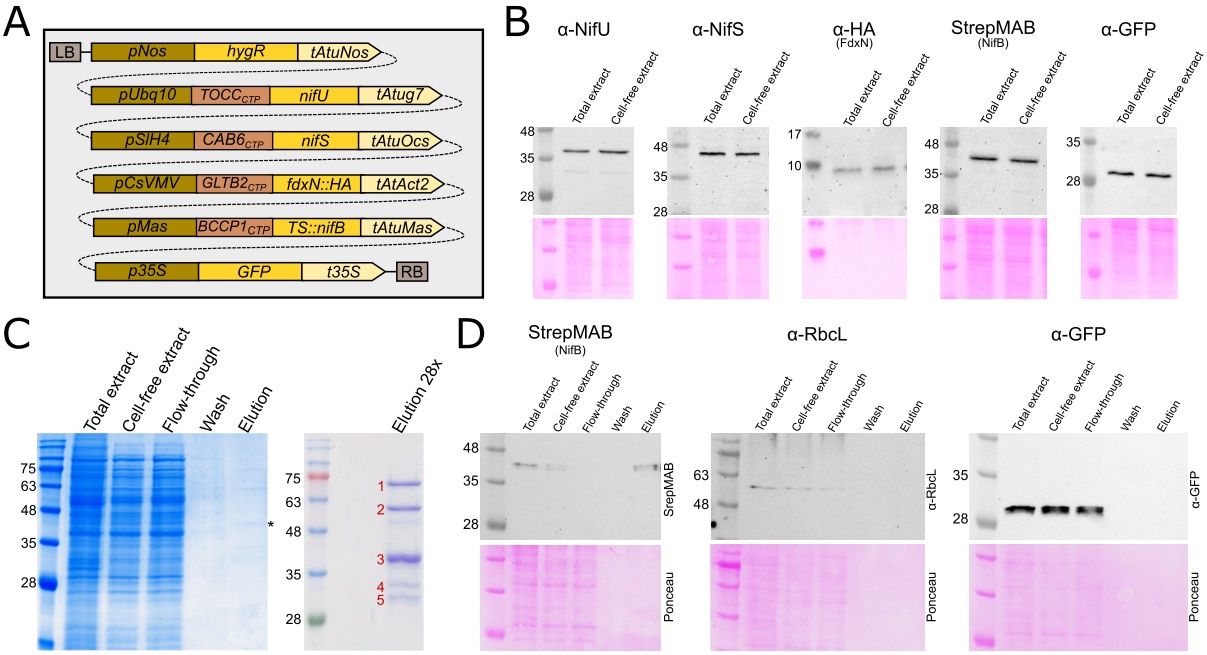

Fig 6: Multi-gene stacking of the NifB module in stably transformed plant cells. (A) Construct design for stable transformation for expression plastid-targeted NifU, NifS, FdxN::HA, Twin-Strep::NifB, and cytosolic GFP. CTP: chloroplast targeting peptide (B) Western blots and ponceau-stained membranes of total and soluble plant extracts from MM1 plant cells transformed with the construct depicted in (A) with *nifB* from *Methanobacterium bryantii*, using α-NifU, α-NifS, α-HA, α-StrepII and α-GFP antibodies. (C) Left panel: Coomassie-stained SDS-PAGE gel loaded with different fractions of the Strep-Tactin affinity chromatographic purification of Col-0 cells transformed with the construct depicted in (A) with *nifB* from *Methanosarcina acetivorans*. Asterisk indicates the expected mass of TS-NifB, 39.5 kDa. Right panel: concentrated elution. Bands labelled with red numbers were analyzed by mass spectrometry. Band 3 was identified as TS::NifB, whereas bands 1, 2, and 4 corresponded to co-purified Arabidopsis proteins methylcrotonoyl-CoA carboxylase subunits alpha (Q42523) and beta (Q9LDD8), and the biotin carboxyl carrier protein of acetyl-CoA carboxylase (F4KE21), respectively. Band 5 was identified as a mix of the Arabidopsis proteins A0A384KVD0 and Q9SSR9 of unknown functions. (D) Western blots of the purification steps shown in (C) with the α-Strep (StrepMAB), α-RbcL, α-GFP antibodies.